ACS APPLIED POLYMER MATERIALS

pubs.acs.org/acsapm Article

N-Type Complementary Semiconducting Polymer Blends

William W. McNutt, Aristide Gumyusenge, Luke A. Galuska, Zhiyuan Qian, Jiazhi He, Xiaodan Gu, and Jianguo Mei*

Cite This: *ACS Appl. Polym. Mater.* 2020, 2, 2644−2650 Read Online

ACCESS | Metrics & More | Article Recommendations | Supporting Information

ABSTRACT: Complementary semiconducting polymer blends (*c*-SPBs) have been demonstrated as an effective approach to balance performance and processing of semiconducting polymers for organic field-effect transistors. All previously reported *c*-SPBs have been exclusively based on p-type polymers. In this report, we designed and synthesized naphthalene diimide (NDI) based matrix polymers and systematically studied n-type charge transport behaviors of their corresponding polymer blends. NDI-C_m (m = 3−7) polymers displayed low melting points (55−105 °C) allowing for the lowest temperature melt-processing of organic transistors to date with mobilities up to 1.01×10^{-3} cm^2 V^{-1} s^{-1}. NDI-C_m polymers were revealed to be nearly amorphous by GIXRD and thin film UV−vis which explain the lowered thermal transitions and observed poor charge transport. Utilizing a *c*-SPB with 5% fully conjugated P(NDI2OD-T2), the transistor performance improved up to 100-fold of the pure matrix polymer despite the low crystallinity of NDI-C_m thin films.

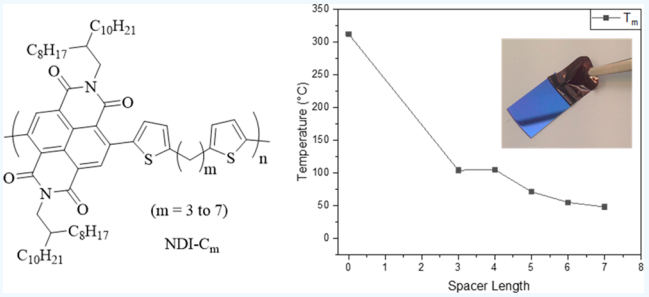

KEYWORDS: *melt processing, semiconducting polymers, backbone engineering, organic field effect transistors, n-type, polymer blends*

INTRODUCTION

Semiconducting polymers have gained attention because of their wide application potential in solar cells, light-emitting diodes, transistors, and other devices.[1−3] Organic semiconducting polymers are conceivably more mechanically conformable and lightweight than their inorganic counterparts and can be fabricated from solutions with fast printing techniques such as inkjet printing and slot-die coating.[4,5] Organic semiconductors are held together by secondary forces (van der Waals force), and the weak intermolecular interactions render these polymers to have poor charge transport characteristics.[6] The focus in the field has mainly been to improve the electrical performance of conjugated polymers which initially was significantly lower than inorganic materials. The performance of semiconducting polymers has steadily increased over time and is now comparable and superior to amorphous silicon.[7] Unfortunately, most of the early developed high-performance semiconducting polymers are only soluble and processed from toxic chlorinated solvents.[8] Sometimes, it even requires processing them under high temperatures.[9] Thus, it virtually makes them incompatible with environmental standards and industrial manufacturing processes. There are a variety of efforts to improve the processability of semiconducting polymers, ranging from molecular design (i.e., side chain engineering and precursor method) to process engineering (i.e., the formation of nanoparticles).[10−12] Our group previously focused on a completely different approach and introduced the concept of complementary semiconducting polymer blends (*c*-SPBs).[13−20] *c*-SPBs are composed of a semiconducting matrix polymer with conjugation-break spacers along the polymer backbone and a fully conjugated polymer that functions as a tie chain.[13] With the conjugation break spacers, matrix polymers expectedly present inadequate electrical properties but greatly improve their desired physical properties such as solubility and melt temperature.[17] The blending of the matrix polymer with 1−5% fully conjugated analogue (tie-chain) nearly brings the hole mobility back to that of a fully conjugated polymer. Further, the lowered melting transition of the blends allowed our group to prepare melt-processed organic field-effect transistors (OFETs), eliminating the use of chlorinated solvents.[18] To date, donor−acceptor type polymers containing conjugation break spacers and their corresponding complementary blends have been exclusively demonstrated with p-type charge transport. It is not clear if this blending design strategy can be successfully extended to n-type donor−acceptor type polymers. Facchetti and Yao et al. reported the only known n-type matrix polymer poly[*N*,*N*′-bis(2-octyldodecyl)-1,4,5,8-naphthalenedicarboximide-2,6-diyl]-*alt*-5,5′-[2,2′-(1,2-ethanyl)bithiophene] (P(NDI2OD-TET)) where a

Received: March 13, 2020
Accepted: May 27, 2020
Published: June 10, 2020

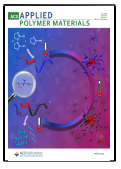

https://dx.doi.org/10.1021/acsapm.0c00261
ACS Appl. Polym. Mater. 2020, 2, 2644−2650

Scheme 1. Synthesis of Monomers and Polymers

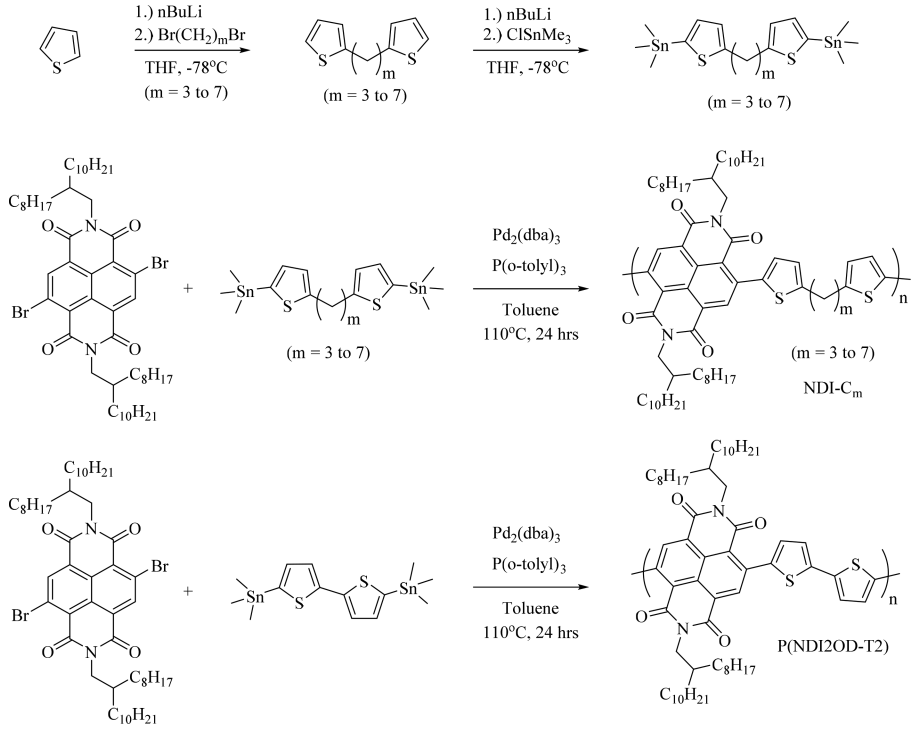

Table 1. Physical Properties of the NDI-C_m and P(NDI2OD-T2) Polymers

				λ_{max}^{abs} (nm)			energy levels (eV)	
polymer	Mn (kDa)/PDI[a]	T_d (°C)[b]	T_m (°C)[c]	soln[d]	thin film[e]	E_g^{opt} (eV)[f]	E_{HOMO}[g]	E_{LUMO}[h]
NDI-C3	50.8/1.6	436	104/60	519	520	2.08	−5.82	−3.74
NDI-C4	21.7/1.9	436	105/76	520	517	2.08	−5.86	−3.78
NDI-C5	12.6/1.4	428	71/54	520	518	2.08	−5.86	−3.77
NDI-C6	18.0/1.3	425	55	520	518	2.08	−5.86	−3.78
NDI-C7	28.6/2.0	425	48	521	520	2.08	−5.86	−3.78
P(NDI2OD-T2)	157.5/2.0[i]	448	312	701	705	1.55	−6.22	−4.69

[a]Tetrahydrofuran (THF) as the eluent at 40 °C. [b]Decomposition temperature. [c]Melting temperature. [d]Chloroform solution. [e]Dropcast films on glass substrates, annealed at 50 °C. [f]Calculated from the onset absorption $E_g^{opt} = 1240/\lambda$ onset abs (nm). [g]Calculated using the equation $E_{HOMO} = E_{LUMO} - E_g^{opt}$. [h]LUMO energy level determined by CV $E_{LUMO} = -[4.8 + (E_{red} - E_{1/2(ferrocene)})]$ eV. [i]1,2,4-trichlorobenzene (TCB) as eluent at 160 °C.

saturated $-CH_2-CH_2-$ group is inserted in between the two thienyl units to break polymer backbone π-conjugation.[21] They studied this polymer and a fully conjugated analog poly[*N*,*N*′-bis(2-octyldodecyl)-1,4,5,8-naphthalenedicarboximide-2,6-diyl]-*alt*-5,5′-(2,2′-bithiophene) (P(NDI2OD-T2)) and found that the spacer had a profound impact on the redox properties and cycling stability in the context of energy storage. In other words, the concept of n-type *c*-SPBs was not validated there. Considering the difference between p-type and n-type charge transport, it thus provides ample motivation to investigate and validate n-type *c*-SPBs performance.

In this study, we prepared five naphthalene diimide (NDI) based matrix polymers (NDI-C_m, m = 3−7) where a conjugation break spacer (CBS) of three to seven methylene groups is inserted into P(NDI2OD-T2). The impact of CBS length on physical, optical, and electrical properties has been fully explored with these NDI-C_m polymers. Further, we studied the blends of NDI-C_m and P(NDI2OD-T2) and their electronic properties in OFETs. The obtained results proved that the concept of n-type *c*-SPBs is valid. Built on this discovery and taking advantage of the low melt transitions of the blends, melt-processed OFETs with n-type *c*-SPBs were fabricated. The blend containing 5 wt % of P(NDI2OD-T2) in NDI-C3 offered averaged electron mobilities up to 0.012 $cm^2 V^{-1} s^{-1}$. The melt processing temperature of 100 °C represented the lowest temperature to obtain melt-processed semiconducting thin films to date. Additionally, thin film morphologies have been probed with atomic force microscopy (AFM) and grazing incidence X-ray diffraction (GIXRD).

RESULTS AND DISCUSSION

Monomer and Polymer Synthesis. Synthetic routes for the NDI-C_m polymers are shown in Scheme 1. The synthesis for the linear methylene CBS monomers were performed as previously reported.[17] Polymers were prepared by Stille coupling polymerization; experimental details can be found in the Supporting Information and Experimental Details. The polymers were then purified by sequential Soxhlet extraction with acetone, hexane, and chloroform. The hexane or chloroform fractions were collected, concentrated, and then precipitated in methanol. The polymers were collected by

https://dx.doi.org/10.1021/acsapm.0c00261
ACS Appl. Polym. Mater. 2020, 2, 2644−2650

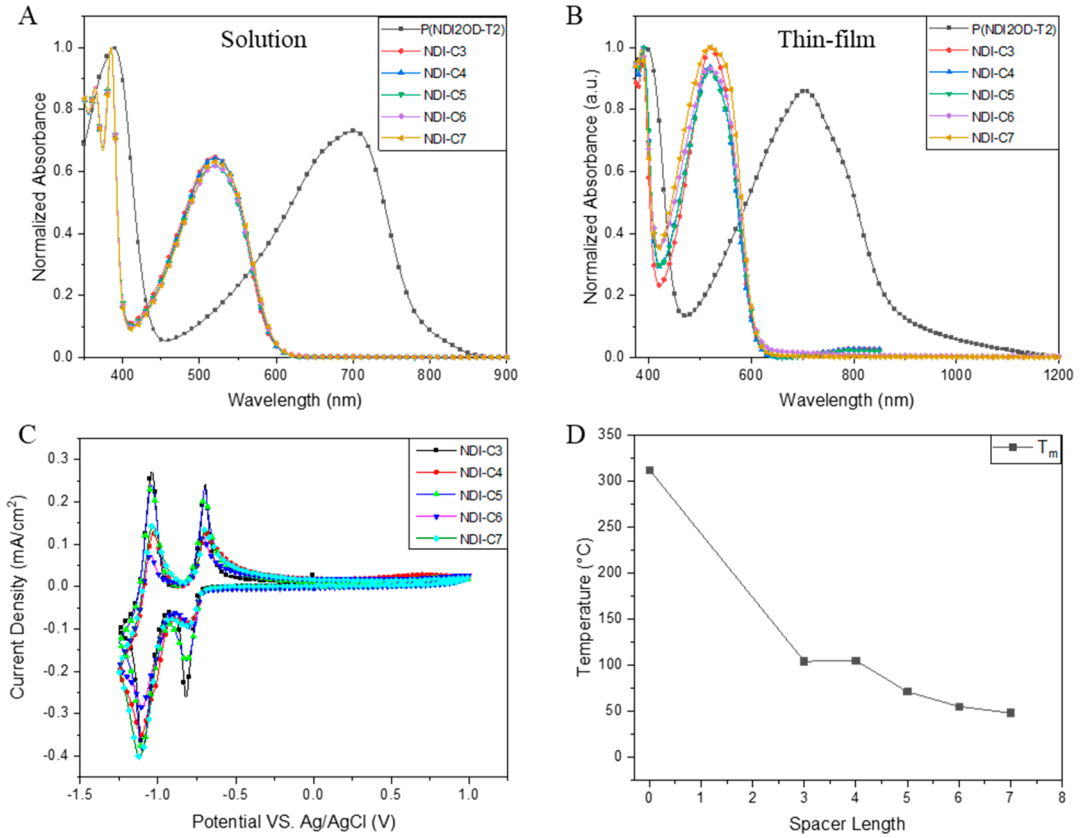

Figure 1. UV−vis spectra of NDI-C_m and P(NDI2OD-T2) Polymers. (A) Chloroform solutions. (B) Thin films. (C) Cyclic voltammetry of NDI-C_m polymers. CV and DPV of P(NDI2OD-T2) are in the SI. (D) Melting point trend of NDI-C_m and P(NDI2OD-T2) polymers. DSC thermograms are in Figure S4.

vacuum filtration and dried under vacuum at elevated temperatures for shorter spacers (3/4); longer spacers (5−7) were dried only under vacuum due low melting points. With increasing CBS length, the solubility of the NDI-C_m polymers noticeably increased, longer spacers (5−7) showed great solubility in hexane even with comparable molecular weights as the shorter spacers containing polymers. The polymers were characterized by ^{1}H NMR and gel permeation chromatography (GPC). Thermal properties were evaluated by thermal gravimetric analysis (TGA) and differential scanning calorimetry (DSC). The optical and electronic properties were determined by UV−vis spectroscopy (UV−vis) and cyclic voltammetry (CV) respectively. The results of the characterizations can be found in Table 1. Molecular weight and polydispersities (PDI) were estimated by GPC with tetrahydrofuran (THF) as the eluent at 40 °C. The molecular weights range from 12.6 to 50.8 kDa with PDIs between 1.4 and 3.4. Due to insolubility in THF, the molecular weight and PDI of P(NDI2OD-T2) were estimated by GPC with 1,2,4-trichlorobenzene (TCB) as the eluent at 160 °C and found to be 157.5 kDaA and 2.0, respectively. ^{1}H NMR of the five matrix polymers gave very sharp peaks, unlike the broad peaks typically observed in polymer systems. This suggests the polymers are completely unaggregated in chloroform solutions.

Polymer Characterizations. The optical properties of the synthesized matrix polymers were evaluated by UV−vis spectroscopy, and the corresponding results are summarized in Table 1. Solution and solid-state spectra are shown in Figure 1. In chloroform solutions all polymers exhibited a high energy transition peak close to 400 nm and a lower energy peak maximum absorption at 520 nm which originates from the isolated π conjugated segment of the matrix polymers. This is in contrast with P(NDI2OD-T2) that shows a significant red-shift due to extended conjugation length. Pure matrix thin films show similar absorbance with no bathochromic shift from π-aggregation as is typically expected from conjugation polymer thin films like that observed in P(NDI2OD-T2). This implies that NDI-C_m polymers are a disordered system. This is in good agreement with GIXRD results shown in Table S1. Energy levels of the matrix polymers were investigated using cyclic voltammetry (CV; Figure 1). All NDI-C_m polymers have two reversible reduction peaks. The first peak is at −0.7 V providing a low lying LUMO level at −3.7 eV. The HOMO levels estimated from $E_{LUMO} - E_g^{opt}$ (Table 1) were found to be −5.82 to −5.86 eV for all matrix polymers. Thermal gravimetric analysis (TGA) and differential scanning calorimetry (DSC) were used to evaluate the thermal properties of the polymers, and the results are summarized in Table 1 and Figure 1D. DSC and TGA thermograms are shown in Figures S3 and S4. All polymers demonstrated excellent thermal stability with no decomposition until around 425 °C. Thermal characterization of NDI-C_m polymers by DSC proved difficult due to the apparent long recrystallization times. The melting points of the polymers were not always observable on the second DSC scans which is typically reported to ensure no influence of thermal history. Melting point transitions are observed to be within 48−102 °C. The melting point decreases with increasing CBS length. NDI-C_m polymers have drastically lowered melting points in comparison with fully conjugated

https://dx.doi.org/10.1021/acsapm.0c00261
ACS Appl. Polym. Mater. 2020, 2, 2644−2650

Table 2. Charge Transport Properties of P(NDI2OD-T2), NDI-C_m, and 5% *c*-SPB Annealed at 100 °C

	pure polymers				5% *c*-SPB
polymer	μ_{eavg} cm^2 V^{-1} s^{-1}	μ_{emax} cm^2 V^{-1} s^{-1}	V_{th} (V)	I_{on}/I_{off}	μ_{emax} cm^2 V^{-1} s^{-1}
NDI-C3	4.02×10^{-4}	1.01×10^{-3}	+23.6	1.02×10^{3}	0.012
NDI-C4	5.13×10^{-5}	2.01×10^{-4}	+20.1	3.19×10^{3}	8.90×10^{-3}
NDI-C5	1.10×10^{-5}	1.3×10^{-5}	+22.1	2.34×10^{3}	1.03×10^{-3}
NDI-C6	$<1.0 \times 10^{-6}$	$<10 \times 10^{-6}$	NA	NA	5.53×10^{-5}
NDI-C7	$<1.0 \times 10^{-6}$	$<10 \times 10^{-6}$	NA	NA	6.30×10^{-5}
P(NDI2OD-T2)	0.098	0.178	+24.0	2.84×10^{2}	

P(NDI2OD-T2). All melting points observed are highly favorable for melt-processing at low temperatures.

Charge Transport Properties of Matrix Polymers and *c*-SPBs. The charge transport characteristics of pure NDI-C_m (m = 3−7) and their 5% *c*-SPBs were evaluated using field-effect transistor devices in a bottom-gate, bottom contact configuration. Pure matrix polymer thin films were prepared by melt processing as previously reported apart from lower processing temperature at 100 °C.[14] For *c*-SPB thin films, the matrix polymers and 5% tie-chain (P(NDI2OD-T2) were premixed in solution, and the dried mixed pellets were used to fabricate the transistor devices. Average mobilities were extracted from 20 different devices for all the studied polymers.

For all matrix polymers only n-type transport was observed in contrast to P(NDI2OD-T2) which demonstrates ambipolar behavior (Figures S10 and S13). The measured electron mobility from the matrix polymers was strongly diminished with insertion of conjugation break spacers and continued to rapidly decrease with length. Only shorter spacer length (3−5) demonstrated measurable mobility while with longer spacer lengths of 6/7, the mobility was near the limit of detection. This was in good agreement with the previously reported DPP system.[17] The low mobilities were also in good agreement with the low crystallinity and weak $\pi-\pi$ aggregation displayed by the matrix polymers in GIXRD and UV−vis respectively, as well as the high lying LUMO level shown by CV. The extracted OFETs results are summarized in Table 2, and representative characteristic transfer curves are shown in Figure S10. It should be noted that these devices were tested in the air for comparison with the parent tie-chain despite the inherent sensitivity of n-type materials toward oxygen and moisture. It was thus encouraging that, even with methylene units inserted to break the backbone conjugation, these matrix polymers could still exhibit extractable charge mobilities. Unlike previously reported DPP-C_m polymers, NDI-C_m polymers display no odd−even effect trend in mobility.[17]

With these matrix polymers in hand, we investigate complementary semiconducting polymer blends, an approach that has been demonstrated by our research group as a robust strategy to enhance charge-transport properties of semiconducting matrix polymers.[13,14,16−19] This method has yet to be demonstrated with n-type materials. To test the validity of *c*-SPBs for n-type matrix polymers, we blended 5 wt % of the fully conjugated P(NDI2OD-T2) (tie-chain) parent polymer with the matrix polymer. This led to an improvement of up to 100-fold for n-type charge transport for NDI-C5. In the case of NDI-C3 5% blend, a record high electron mobility among n-type, melt-processed polymers, 0.012 cm^2 V^{-1} s^{-1}, could be obtained from the melt processed blend films. When the conjugation break spacer length was further increased, the blending efficiency could only boost the charge mobilities to moderate values as shown in Table 2. This could be partly due to the lack of crystallinity in the matrix polymer as, *c*-SPBs rely on the tie chain polymer interconnecting the crystalline domains to achieve effective charge mobility. Since the increase in the spacer length shows to lower the matrix' crystallinity, we would expect the blending effect to start declining. Further increase in the P(NDI2OD-T2) content of the blends showed to only moderately increase the mobility (Figure S13) as predicted from the complementary blending design that charge mobility will begin to plateau (Figure 2).[13]

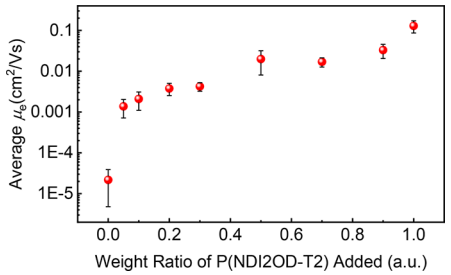

Figure 2. N-type mobility trend for NDI-C5 *c*-SPBs with increasing P(NDI2OD-T2) content.

Morphology and Molecular Packing Information. Thin film morphology characterizations and molecular packing studies were carried out to probe the charge transporting pathways in the fabricated OFETs devices. Atomic force microscopy (AFM) was used to characterize solid-state morphologies, and grazing incidence X-ray diffraction (GIXRD) for the molecular packing in thin films. AFM images (Figure S5) revealed smooth surface morphology for all the NDI-C_m polymers. These morphologies came to support the shiny metallic luster observed at the microscale from the melt-pressed films (Figure 3c). This smoothness was showed to increase when the films were treated to temperatures higher than their corresponding melting points. The smoothness of all thin films allow for easy delamination from the substrate into free-standing thin films. All thin films could easily be transferred and laminated onto prepatterned substrates for OFET fabrication. This lack of any large surface aggregates in thin films could also support the nonaggregation seen in the UV−vis spectra. In contrast, pure spin-cast thin films of the rigid fully conjugated tie-polymer P(NDI2OD-T2) showed large aggregates (Figure 3), in accordance to its red-shifted UV−vis maximum absorption. No notable morphological changes were observed when it was treated at the same temperatures as the matrices. The tie-polymer did not show signs of melting until 300 °C in accordance to the DSC results. For *c*-SPBs, a significant morphology change could be observed when only 5% of the tie-chain polymer was used. In comparison to pure NDI-C5, for instance, the thin films became much rougher indicative of solid-state aggregate

https://dx.doi.org/10.1021/acsapm.0c00261
ACS Appl. Polym. Mater. 2020, 2, 2644−2650

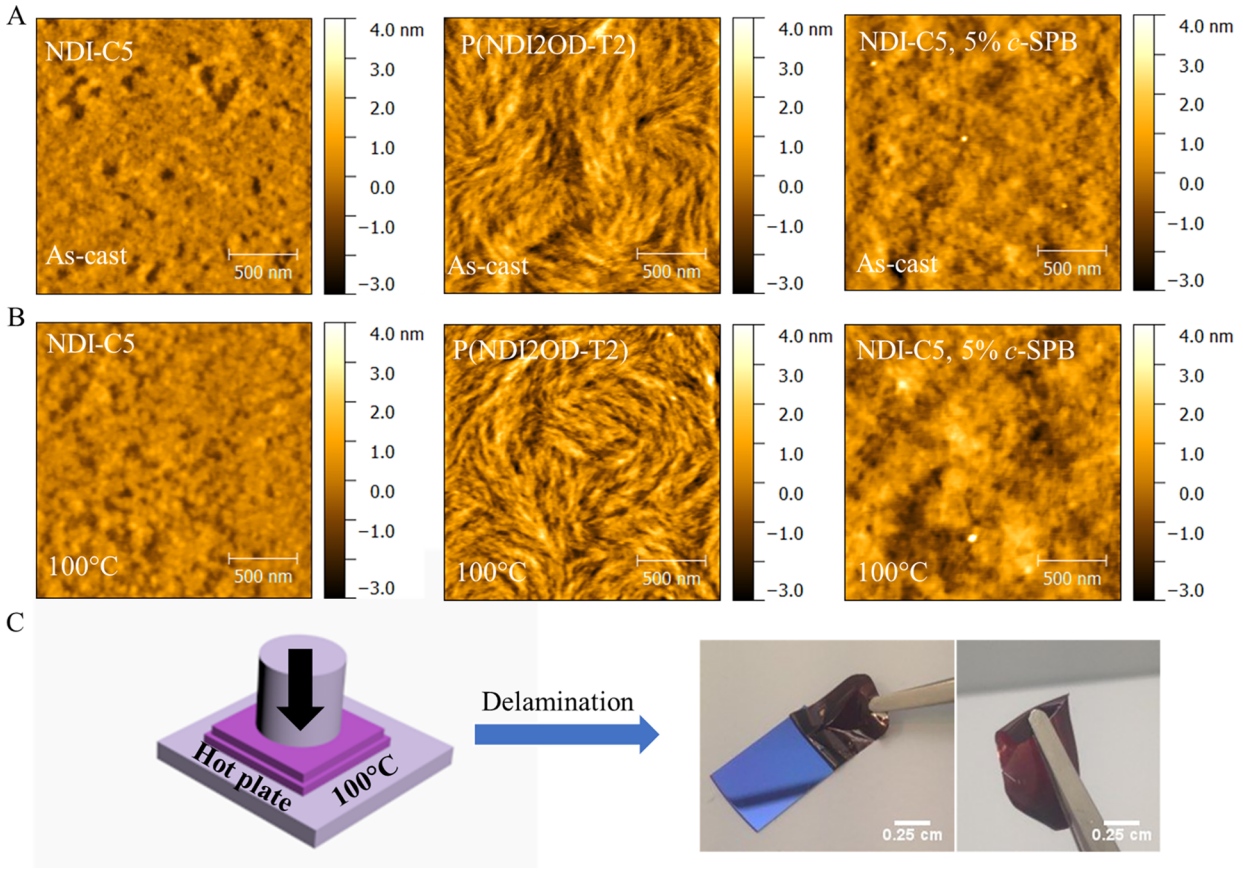

Figure 3. (A) AFM images of NDI-C5, P(NDI2OD-T2), and NDI-C5 5% *c*-SPB thin films as cast. (B) Images of the same thin films after annealing at 100 °C to show that NDI-C5 and 5% *c*-SPB melted into smoother films for delamination. (C) Technique demonstration of melt-processing bulk polymer material into thin films and subsequent delamination.

formation (Figure 3). Increasing the content of the tie-chain P(NDI2OD-T2) lead to gradually rougher surface film morphologies (Figure S6) which could support the gradual increase in corresponding mobilities. The thin film surfaces do not show signs of phase segregation like previously reported systems.

GIXRD results of the matrices revealed low crystallinity for the studied matrices in comparison to the fully conjugated analogue. Weak lamellar stacking could be observed in the out-of-plane directions for NDI-C$_m$ thin films. No strong $\pi-\pi$ stacking could be found for the matrices, and these results were not surprising due to the low charge carrier mobilities observed. P(NDI2OD-T2) showed a clear predominantly face-on orientation with a strong $\pi-\pi$ stacking signal in the out-of-plane signal. The contribution of this packing to the blends containing a small portion of P(NDI2OD-T2) was also evident, and a $\pi-\pi$ stacking peak started to evolve in the blends. Figures S7 and 8 show the GIXRD 2D patterns of P(NDI2OD-T2), the matrix polymers, and the corresponding 5% *c*-SPBs. A careful extraction of the peak positions was carried out to probe the influence of spacer length on the packing behavior as well as the impact of the rigid tie chains on the blends. The extracted peak positions and intensities are summarized in Table S2, and the corresponding 1D linecuts can be found in the Supporting Information. A Gaussian fitting was performed to evaluate peak intensities. Despite the weakly diffracting nature of the blend films, the impact of having a small percentage of tie-chains within the blends showed initiation of the formation of charge-carrying aggregates within the predominantly amorphous matrices. This approach is thus sought after as a mean to enhance charge transport in n-type polymer systems.

CONCLUSION

In summary, we have prepared and characterized a set of 5 NDI-C$_m$ (m = 3–7) matrix polymers containing CBSs from 3 to 7 methylene units. DSC revealed low melting points more suitable for melt-processing temperatures. The low melting point can be attributed to the lack of crystallinity and π-aggregation as revealed by GIXRD and UV–vis measurements and ^{1}H NMR. The first melt-processed n-type complementary semiconducting polymer blends were demonstrated. Performance of NDI-C$_m$ polymer transistors could be increased up to 100-fold by blending with 5% P(NDI2OD-T2) tie-chain polymer. *c*-SPBs continue to be an emerging method for tailoring both physical and electrical properties of organic thin film transistors. Mechanical properties are currently underway to characterize the apparent ductile nature of these new polymers.

EXPERIMENTAL DETAILS

Materials and Characterizations. All reagents and starting materials were purchased from Sigma-Aldrich and SunaTech and used without further purification. ^{1}H NMR spectra were recorded using Bruker ARX 400 at 293 K with deuterated chloroform as solvent. For NDI-C$_m$ polymers, room temperature gel permeation chromatography (GPC) was performed in tetrahydrofuran under room temperature with a Polymer Laboratories PL-GPC20. The molecular weights of

https://dx.doi.org/10.1021/acsapm.0c00261
ACS Appl. Polym. Mater. 2020, 2, 2644–2650

matrix polymers were calculated using a calibration curve based on polystyrene standards. An Agilent PL-GPC-220 system high temp (HT)-GPC was utilized to characterize the molecular weights of P(NDI2OD-T2) in this study. This system is equipped with 3 pLGel Olexis (13 μm particle size) in series in addition to a differential refractive index (RI) detector, a dual angle (15° and 90°) light scattering (LS) detector, and a viscometer (VS) detector. Prior to the GPC analysis, the polymers were dissolved by shaking in 1,2,4-trichlorobenzene (TCB) at a concentration of 1−2 mg/mL for 2 h at 160 °C and subsequently filtered through a 2 μm stainless steel filter. All polymers were run in the instrument at 160 °C using TCB as an eluent. The chromatograms were worked up from the RI signal utilizing a narrow standard polystyrene calibration (14 points, ranging from 162 g/mol to 3 242 000 g/mol). TGA measurements were carried out on a Mettler-Toledo TGA/DSC 3+ equipped with a Huber minichiller 300 under a nitrogen gas purge rate of 50 mL/min. The samples were heated from 25 to 700 °C at a heating rate of 10 °C/min. A Mettler-Toledo DSC 3+ equipped with a FRS6+ sensor and a Huber TC100 intracooler was utilized for DSC measurements, under a dry nitrogen gas purge with a flow rate of 50 mL/min. A heat−cool−heat cycle with rate of 30 °C/min was applied. UV−vis−NIR spectra were recorded on a Cary 50 spectrophotometer (350−1200 nm). Atomic force microscopy images were obtained on a Veeco Dimension 3100 AFM in tapping mode. GIWAXS were performed at a sample to detector distance of ∼ 300 mm under a helium environment with an incident beam energy of 12.7 keV and an incidence angle of 0.12°. The data was collected on beamline 11-3 at the Stanford Synchrotron Radiation Lightsource. The analysis was performed using Nika software package within Wavemetrics Igor, in combination with WAXS tools. The cyclic voltammetry (CV) experiments were performed in a three-electrode cell with a scan rate of 40 mV/s. The working electrode was the platinum bottom electrode coated with NDI polymers; the reference electrode was a leakless Ag/AgCl electrode; the counter electrode is the platinum wire; and the electrolyte is 0.2 M $TBAPF_6$ in propylene carbonate.

Thin Film Formation and Device Characterization Methods. Materials P(NDI2OD-T2) (3.3 mg/mL) and NDI-C_m (10 mg/mL) were dissolved in chloroform at 50 °C stirred overnight. The *c*-SPB solutions were obtained by mixing the X wt % of P(NDI2OD-T2) solutions into (100 − X) wt % NDI-C_m solutions. Before use, the P(NDI2OD-T2) solution was stirred and heated up to 50 °C. The *c*-SPB solid was dried from its solutions.

OFET Device Fabrication. OEFT device fabrication and octadecyltrichlorosilane (OTS) modification were performed as previously reported.[17]

Melt-Processed Thin Film Fabrication. Solution-based OTS-modification was used to prepare the substrates for melt processing. The NDI-C_m and *c*-SPB materials are sticky to glass or bare silicon wafer and hard to peel-off, thus the OTS-modification is essential for the peel-off process. For film fabrication, the NDI-C_m or *c*-SPB materials were put between to OTS-modified substrates on a hot plate. After the materials are melted, a heavy object (∼4 kg) was placed on top of the substrates to press the materials. With different press times and temperatures, different film thicknesses can be achieved. For the peel-off process, the two substrates were first separated. The film was then peeled off, starting from the corner or the edge of the substrate.

Electrical Characterization. Device characterization was carried out using Keithley 4200 in ambient air for all devices. For hot-pressed *c*-SPB OFETs, the electrical measurement was carried out at room temperature in ambient air. The field-effect mobility was calculated in the saturation regime by using the equation $I_{DS} = (\mu W C_i/2L)(V_G - V_T)^2$, where I_{DS} is the drain−source current, μ is the field-effect mobility, W is the channel width, L is the channel length, C_i is the capacitance per unit area of the gate dielectric layer, V_G is the gate voltage, and V_T is the threshold voltage. Three batches of devices and more than five devices in each batch were tested, and their results were in good agreement.

■ ASSOCIATED CONTENT

Supporting Information

The Supporting Information is available free of charge at https://pubs.acs.org/doi/10.1021/acsapm.0c00261.

Characterization details and additional experimental data (PDF)

■ AUTHOR INFORMATION

Corresponding Author

Jianguo Mei − *Department of Chemistry and Birck Nanotechnology Center, Purdue University, West Lafayette, Indiana 47907, United States;* orcid.org/0000-0002-5743-2715; Email: jgmei@purdue.edu

Authors

William W. McNutt − *Department of Chemistry, Purdue University, West Lafayette, Indiana 47907, United States*

Aristide Gumyusenge − *Department of Chemistry, Purdue University, West Lafayette, Indiana 47907, United States*

Luke A. Galuska − *School of Polymer Science and Engineering, The University of Southern Mississippi, Hattiesburg, Mississippi 39406, United States*

Zhiyuan Qian − *School of Polymer Science and Engineering, The University of Southern Mississippi, Hattiesburg, Mississippi 39406, United States*

Jiazhi He − *Department of Chemistry, Purdue University, West Lafayette, Indiana 47907, United States*

Xiaodan Gu − *School of Polymer Science and Engineering, The University of Southern Mississippi, Hattiesburg, Mississippi 39406, United States;* orcid.org/0000-0002-1123-3673

Complete contact information is available at: https://pubs.acs.org/10.1021/acsapm.0c00261

Funding

This work was supported by the NSF CAREER Award (NSF DMR/Polymer, no. 1653909).

Notes

The authors declare no competing financial interest.

■ ACKNOWLEDGMENTS

Part of this work performed by Z.Q., L.A.G., and X.G. was supported by the NSF Office of Integrative Activities no. 1757220. L.A.G. was partially supported by National Science Foundation Division of Graduate Education (DGE) no. 1449999. The authors would also like to thank the Alexander Ayzner group for performing the initial GIXRD measurements. W.W.M. and J.M. are grateful for the financial support from the National Science Foundation Polymer Program (no. 1653909).

■ REFERENCES

(1) Dimitrakopoulos, C. D.; Malenfant, P. R. L. Organic Thin Film Transistors for Large Area Electronics. *Adv. Mater.* **2002**, *14* (2), 99−117.

(2) Forrest, S. R. The path to ubiquitous and low-cost organic electronic appliances on plastic. *Nature* **2004**, *428* (6986), 911−918.

(3) Facchetti, A. π-Conjugated Polymers for Organic Electronics and Photovoltaic Cell Applications. *Chem. Mater.* **2011**, *23* (3), 733−758.

(4) Maunoury, J. C.; Howse, J. R.; Turner, M. L. Melt-Processing of Conjugated Liquid Crystals: A Simple Route to Fabricate OFETs. *Adv. Mater.* **2007**, *19* (6), 805−809.

(5) Baklar, M. A.; Koch, F.; Kumar, A.; Domingo, E. B.; Campoy-Quiles, M.; Feldman, K.; Yu, L.; Wobkenberg, P.; Ball, J.; Wilson, R.

M.; McCulloch, I.; Kreouzis, T.; Heeney, M.; Anthopoulos, T.; Smith, P.; Stingelin, N. Solid-State Processing of Organic Semiconductors. *Adv. Mater.* **2010**, *22* (35), 3942−3947.
(6) Quinn, J. T. E.; Zhu, J.; Li, X.; Wang, J.; Li, Y. Recent progress in the development of n-type organic semiconductors for organic field effect transistors. *J. Mater. Chem. C* **2017**, *5* (34), 8654−8681.
(7) Sirringhaus, H. 25th Anniversary Article: Organic Field-Effect Transistors: The Path Beyond Amorphous Silicon. *Adv. Mater.* **2014**, *26* (9), 1319−1335.
(8) Brandão, L.; Viana, J.; Bucknall, D. G.; Bernardo, G. Solventless processing of conjugated polymers—A review. *Synth. Met.* **2014**, *197*, 23−33.
(9) Sui, Y.; Deng, Y.; Du, T.; Shi, Y.; Geng, Y. Design strategies of n-type conjugated polymers for organic thin-film transistors. *Materials Chemistry Frontiers* **2019**, *3* (10), 1932−1951.
(10) Mei, J.; Bao, Z. Side Chain Engineering in Solution-Processable Conjugated Polymers. *Chem. Mater.* **2014**, *26* (1), 604−615.
(11) Uemura, T.; Mamada, M.; Kumaki, D.; Tokito, S. Synthesis of Semiconducting Polymers through Soluble Precursor Polymers with Thermally Removable Groups and Their Application to Organic Transistors. *ACS Macro Lett.* **2013**, *2* (9), 830−833.
(12) Wu, J.; You, L.; Lan, L.; Lee, H. J.; Chaudhry, S. T.; Li, R.; Cheng, J.-X.; Mei, J. Semiconducting Polymer Nanoparticles for Centimeters-Deep Photoacoustic Imaging in the Second Near-Infrared Window. *Adv. Mater.* **2017**, *29* (41), 1703403.
(13) Zhao, Y.; Zhao, X.; Roders, M.; Qu, G.; Diao, Y.; Ayzner, A. L.; Mei, J. Complementary Semiconducting Polymer Blends for Efficient Charge Transport. *Chem. Mater.* **2015**, *27* (20), 7164−7170.
(14) Gumyusenge, A.; Zhao, X.; Zhao, Y.; Mei, J. Attaining Melt Processing of Complementary Semiconducting Polymer Blends at 130 °C via Side-Chain Engineering. *ACS Appl. Mater. Interfaces* **2018**, *10* (5), 4904−4909.
(15) Xue, G.; Zhao, Y.; Zhao, X.; Li, H.; Mei, J. Zone-Annealing-Assisted Solvent-Free Processing of Complementary Semiconducting Polymer Blends for Organic Field-Effect Transistors. *Advanced Electronic Materials* **2018**, *4* (1), 1700414.
(16) Zhao, X.; Xue, G.; Qu, G.; Singhania, V.; Zhao, Y.; Butrouna, K.; Gumyusenge, A.; Diao, Y.; Graham, K. R.; Li, H.; Mei, J. Complementary Semiconducting Polymer Blends: Influence of Side Chains of Matrix Polymers. *Macromolecules* **2017**, *50* (16), 6202−6209.
(17) Zhao, X.; Zhao, Y.; Ge, Q.; Butrouna, K.; Diao, Y.; Graham, K. R.; Mei, J. Complementary Semiconducting Polymer Blends: The Influence of Conjugation-Break Spacer Length in Matrix Polymers. *Macromolecules* **2016**, *49* (7), 2601−2608.
(18) Zhao, Y.; Zhao, X.; Roders, M.; Gumyusenge, A.; Ayzner, A. L.; Mei, J. Melt-Processing of Complementary Semiconducting Polymer Blends for High Performance Organic Transistors. *Adv. Mater.* **2017**, *29* (6), 1605056.
(19) Zhao, Y.; Zhao, X.; Zang, Y.; Di, C.-A.; Diao, Y.; Mei, J. Conjugation-Break Spacers in Semiconducting Polymers: Impact on Polymer Processability and Charge Transport Properties. *Macromolecules* **2015**, *48* (7), 2048−2053.
(20) Zhao, Y.; Gumyusenge, A.; He, J.; Qu, G.; McNutt, W. W.; Long, Y.; Zhang, H.; Huang, L.; Diao, Y.; Mei, J. Continuous Melt-Drawing of Highly Aligned Flexible and Stretchable Semiconducting Microfibers for Organic Electronics. *Adv. Funct. Mater.* **2018**, *28* (4), 1705584.
(21) Liang, Y.; Chen, Z.; Jing, Y.; Rong, Y.; Facchetti, A.; Yao, Y. Heavily n-Dopable π-Conjugated Redox Polymers with Ultrafast Energy Storage Capability. *J. Am. Chem. Soc.* **2015**, *137* (15), 4956−4959.

https://dx.doi.org/10.1021/acsapm.0c00261
ACS Appl. Polym. Mater. 2020, 2, 2644−2650